SUPPLEMENTARY DATA FILE

Monomeric YoeB toxin retains RNase activity but adopts an obligate dimeric form for thermal stability

Ian Pavelich[1,2,3,4], Tatsuya Maehigashi[1,4], Eric Hoffer[1,2], Ajchareeya Ruangprasert[1], Stacey J. Miles[1], and Christine M. Dunham[1,2,*]

[1]Department of Biochemistry and the [2]Emory Antibiotic Resistance Center, Emory University School of Medicine, Atlanta, Georgia, 30322, [3]Department of Chemistry, Emory University, Atlanta, Georgia, 30322

[4]These authors contributed equally.

*To whom correspondence should be addressed: Tel: 1-404-712-1756; Fax: 1-404-727-2738; Email: christine.m.dunham@emory.edu

Coordinates and structure factors were deposited in Protein Data Bank under accession codes 6NY6, 6OXA, 6OTR, 6OXI.

Running title: Dimeric YoeB toxin is thermal stable

Keywords: toxin-antitoxin complexes, bacterial stress response, ribosome, RNases, heat shock

SUPPLEMENTARY FIGURES

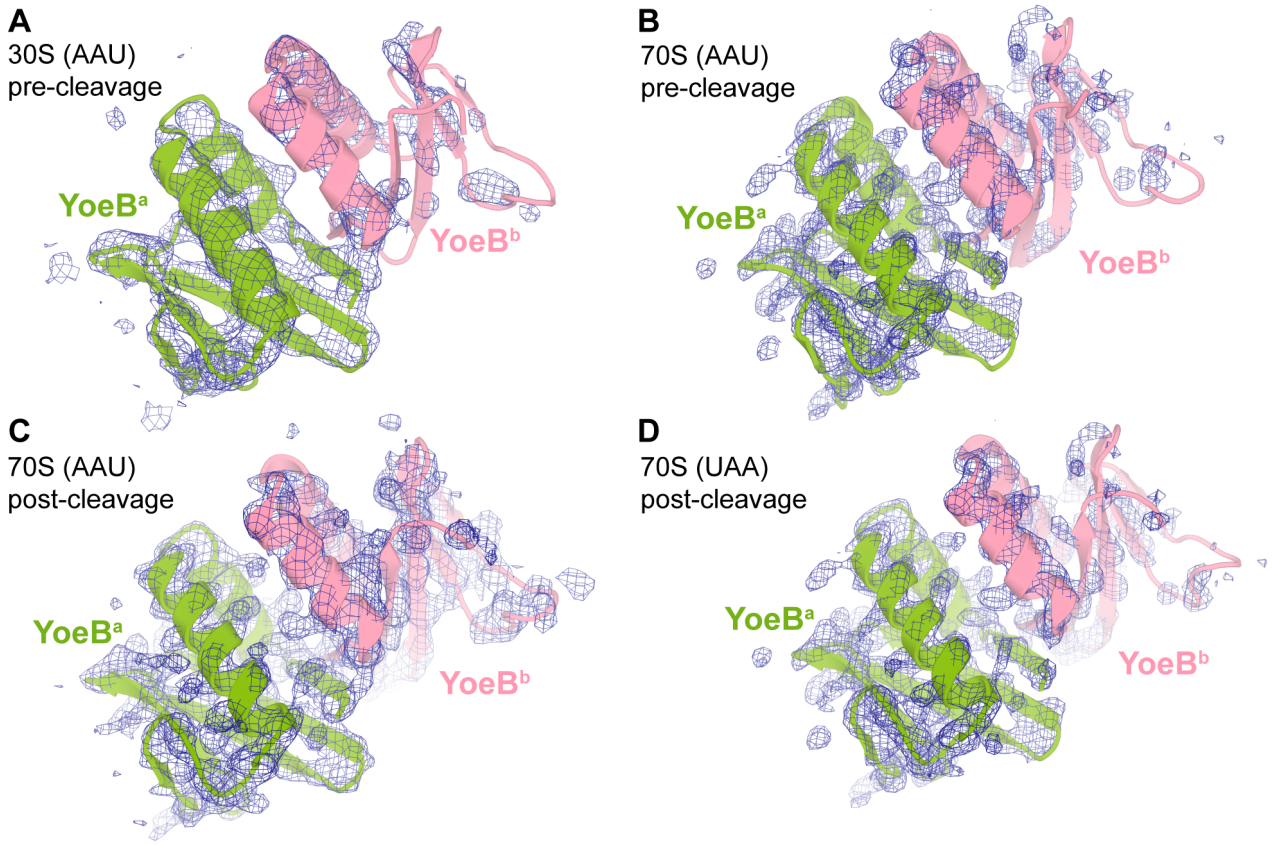

Figure S1. Electron density maps of YoeB bound to the ribosome. (A) $2F_o$-F_c electron density maps (contoured at 1σ) for the YoeB dimer (green and pink) is shown for the 3.7-Å x-ray crystal structure of 30S-YoeB (PDB ID 6NY6); **(B)** the 3.2-Å x-ray crystal structure of 70S-YoeB bound to the A-site AAU asparagine codon in a pre-cleavage state (PDB ID 6OXA); **(C)** the 3.1-Å x-ray crystal structure of the 70S-YoeB bound to the A-site AAU asparagine codon in a post-cleavage state (PDB ID 6OTR); and **(D)** the 3.5-Å x-ray crystal structure of 70S-YoeB post-cleavage state containing an A-site UAA stop codon (PDB ID 6OXI).

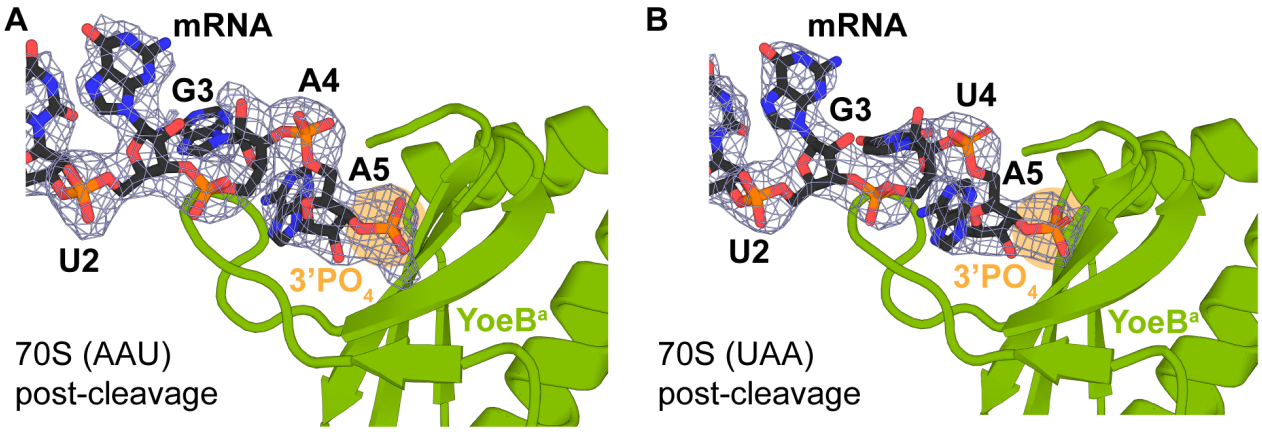

Figure S2. YoeB-mediated mRNA cleavage results in a 3'-phosphate. (A) A 3.1-Å x-ray crystal structure of 70S-YoeB bound to an A-site AAU asparagine codon in a post-cleavage state is shown (PDB ID 6OTR). $2F_o$-F_c electron density map (contoured to 1σ) for mRNA (black) in the A site is shown. The 3'-phosphate resulting from cleavage between the second and third nucleotides of the A-site codon (after A5) is circled in orange. **(B)** A 3.5-Å x-ray crystal structure of the 70S-YoeB bound to an UAA stop codon in a post-cleavage state is shown (PDB ID 6OXI).

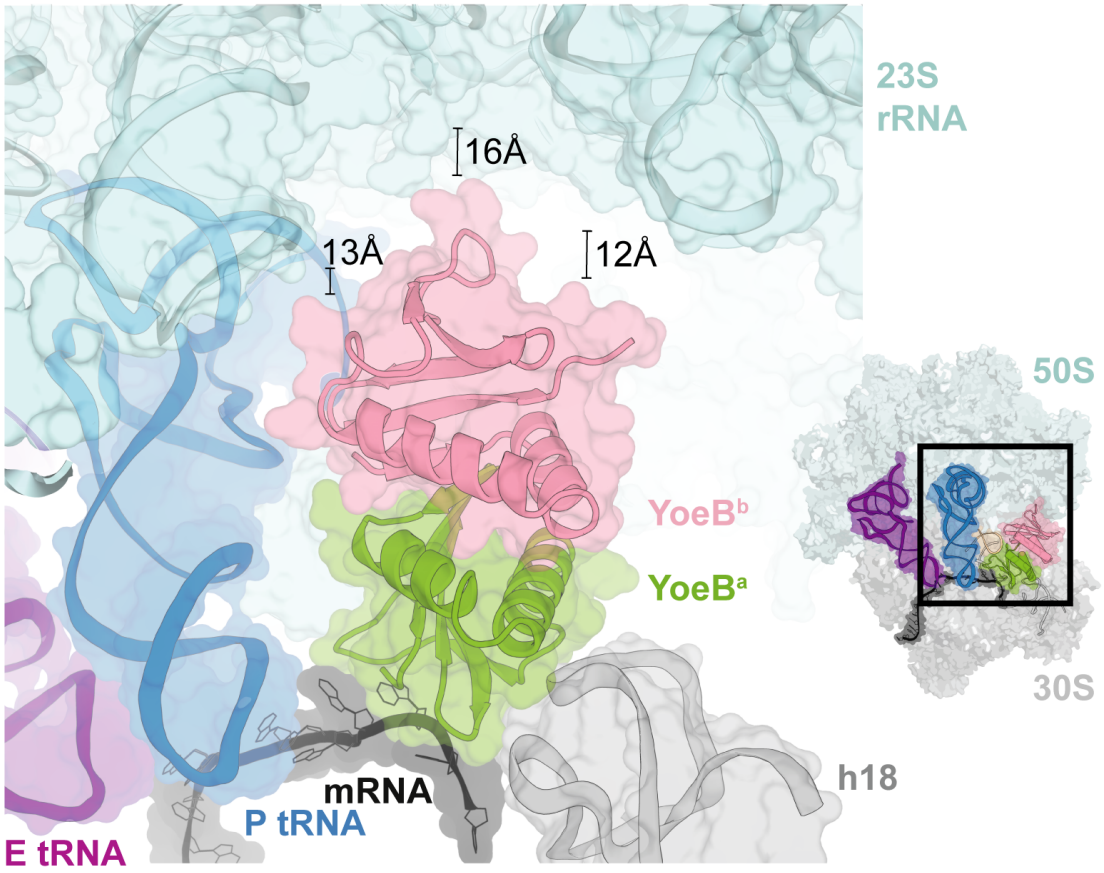

Figure S3. YoeB[b] and the 50S subunit minimally interact. Pre-cleavage structure of dimeric YoeB bound to the *Thermus thermophilus* 70S ribosome containing an AAU codon (50S and 30S subunits are shown as blue and gray, respectively). The closest points of contact between the backbone of YoeB[b] (pink) and 23S rRNA (cyan ribbon and surface) are shown (13 Å, 16 Å, 12 Å). Distances were measured from the Cα of YoeB[b] residues Glu40, His50, and Tyr84, to the backbone phosphate of 23S rRNA nucleotide C885, Cα of ribosomal protein L25 residue Val180, and backbone phosphate of 23S rRNA nucleotide U1066, respectively. P- and E-site tRNAs are shown in blue and purple, respectively. The YoeB monomer closest to the mRNA path is shown in green (YoeB[a]) and the distal YoeB[b] is shown in pink. Inset: A zoomed out figure of the entire ribosomal complex.

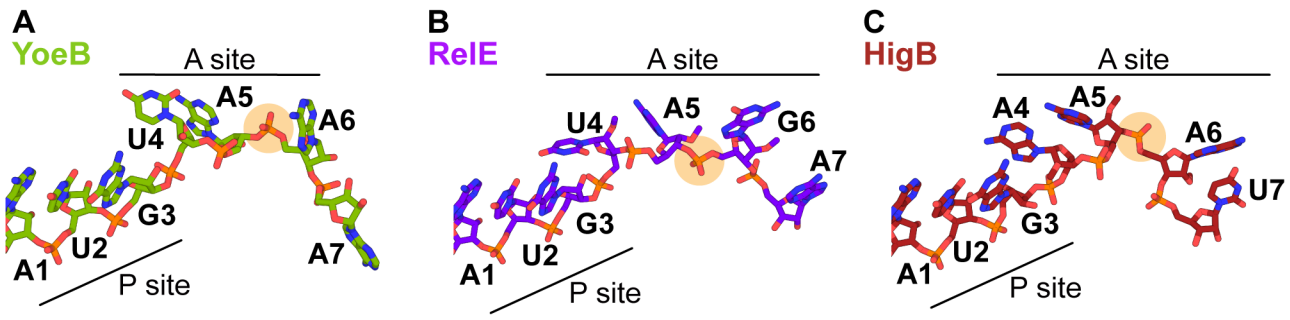

Figure S4. Structural comparison of type II toxins YoeB, RelE, and HigB and their influence on the mRNA path. (A) The location of the mRNA when YoeB binds to the A site (this study, PDB ID 6OXA; YoeB not shown), **(B)** upon RelE binding (PDB ID 4V7J; RelE not shown) and **(C)** upon HigB binding (PDB ID 4YPB; HigB not shown). In each case, the mRNA is re-positioned to expose the scissile phosphate between nucleotides 5 and 6 of the A-site codon. The P-site mRNA nucleotide is labeled starting from +1. The 3'-phosphate resulting from cleavage between the second and third nucleotides of the A-site codon (after A5) is circled in orange.

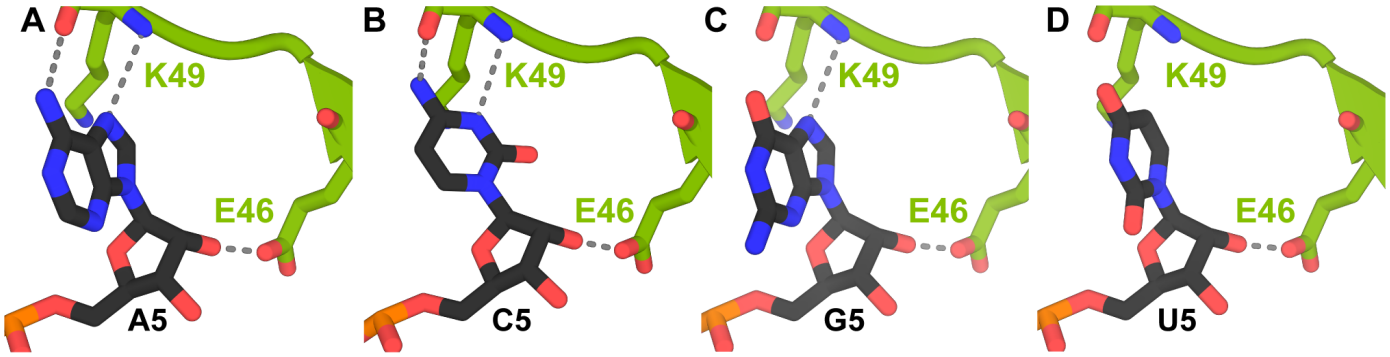

Figure S5. YoeB recognizes either A or C nucleotides at the second position of the mRNA codon. (A) A5 adopts an *anti* conformation to form hydrogen bonds with Glu46 and Lys49, as seen in our 70S-YoeB pre-cleavage state structure bound to a UAA codon. In all panels, YoeB is removed for clarity. **(B)** A model for C5 in an *anti* conformation at the second nucleotide position shows that a cytosine would be able to form the same hydrogen bonding network as in panel (A). **(C)** A model for G5 at the second nucleotide position shows that a guanosine would be unable to form the same hydrogen bonding network as in panel (A). **(D)** A model for U5 at the second nucleotide position shows that an uridine would be being unable to form the same hydrogen bonding network as in panel (A).

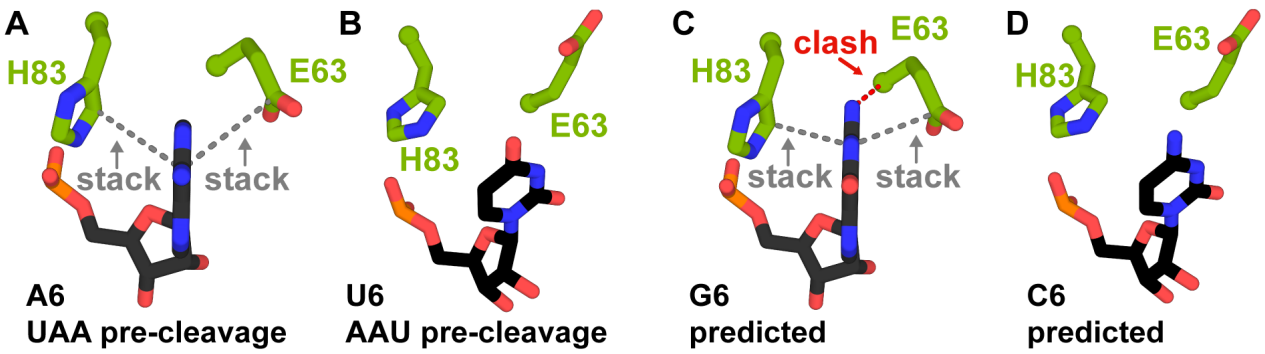

Figure S6. YoeB residues His83 and Glu63 stack with A6, but not U6. (A) In the 70S-UAA pre-cleavage state with remodeled mRNA (1), YoeB[a] residues Glu63 and His83 stack (grey dotted lines) with the A6 nucleobase. **(B)** In the 70S-AAU pre-cleavage state (PDB ID 6OXA), U6 does not form the same stacking interaction as in panel (A). Modeling of position A6 with either **(C)** G6 or **(D)** C6 indicates that a purine, but not pyrimidine, would be able to form the same stacking interaction as in panel (A). The backbone of YoeB near residues Glu63 (β2-3 loop) and His83 (after β4) would have to adjust slightly to avoid a potential steric clash when accommodating a G nucleobase as shown in panel (**C**).

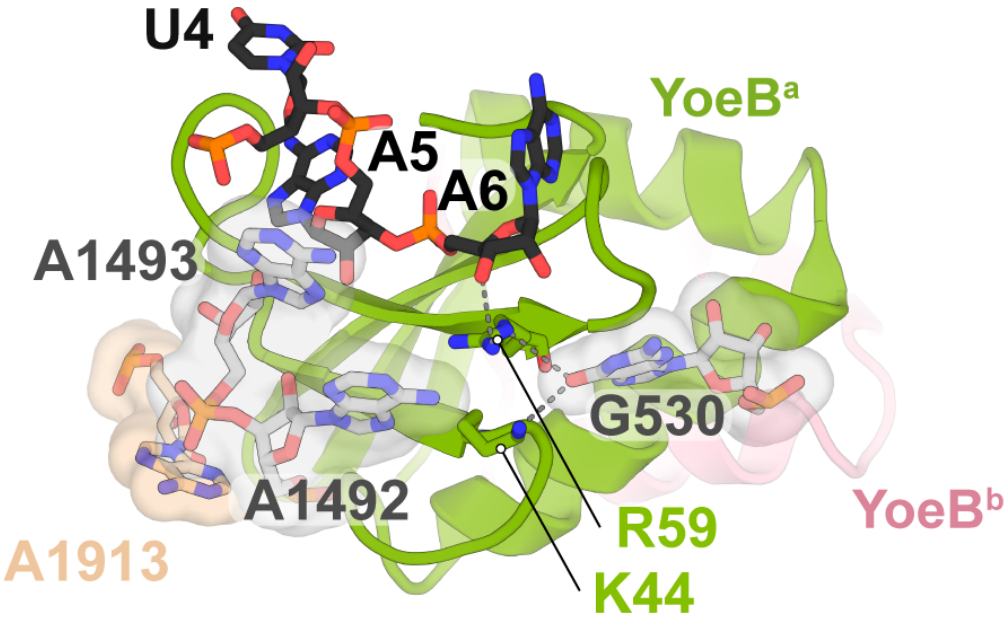

Figure S7. YoeB prevents the interaction between 16S rRNA residues G530 and A1492. YoeB[a] residues Lys44 and Arg59 form a hydrogen bonding network (grey dashed lines) between G530 and A1492, preventing direct interaction. Color scheme is the same as in Figure 1.

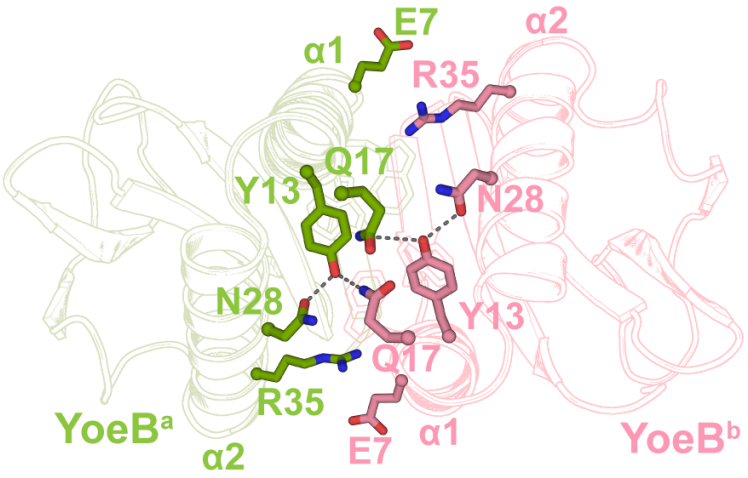

Figure S8. Network of hydrogen bonds between the dimer interface of YoeB[a] and YoeB[b]. YoeB[a] residues (green) that form hydrogen bonds with YoeB[b] residues (pink).

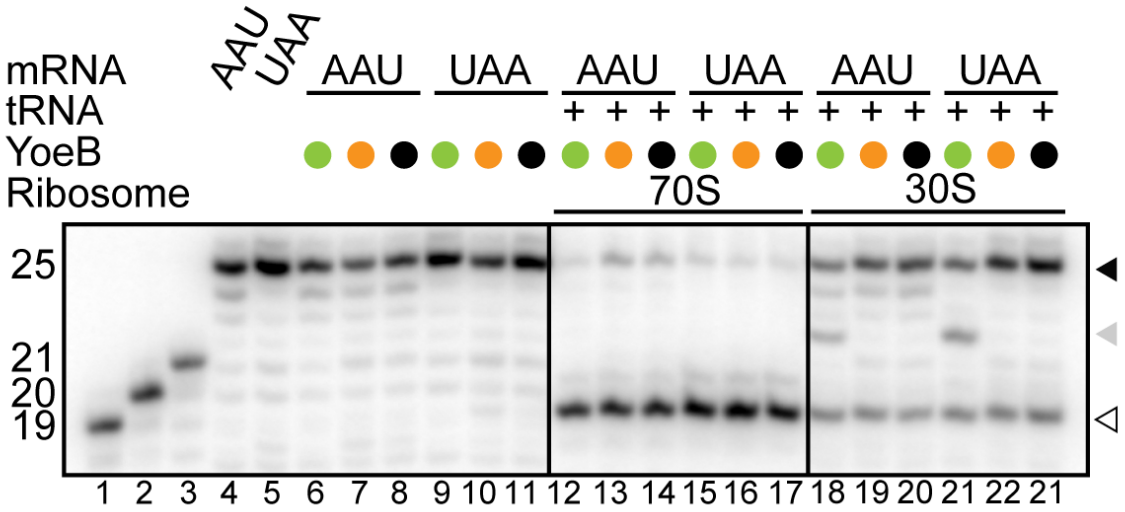

Figure S9. *In vitro* cleavage assays of ^{32}P-labeled mRNA bound to either a 70S or 30S programmed with P-site tRNA^{fMet}. This figure is identical to Figure 6C, except with the addition of control lanes 6-11.The mRNA sequence is the same as shown in Figure 1A. Ribosome complexes were formed as described in the Methods section, YoeB was incubated for 10 mins and reactions were quenched and monitored by denaturing PAGE. Both the AAU and UAA mRNAs are cleaved by YoeB when bound to a 30S and 70S complex (lanes 12-21). YoeB variants W5A and W5A/W10A (denoted as ● and ●, respectively) cleave mRNA bound to either the 30S or 70S as compared to wild-type YoeB (●). Full length mRNA is denoted by a closed arrowhead (▲), cleavage product between the second and the third nucleotide of the mRNA codon by an open arrowhead (△) and the extra mRNA band by a gray arrowhead (▲). 19, 20 and 25-mer mRNA standards are shown in lanes 1-3. Controls with mRNA and YoeB variants alone are shown in lanes 6-11. The line separating the gels indicates each region of the figure were taken from different parts of a single gel.

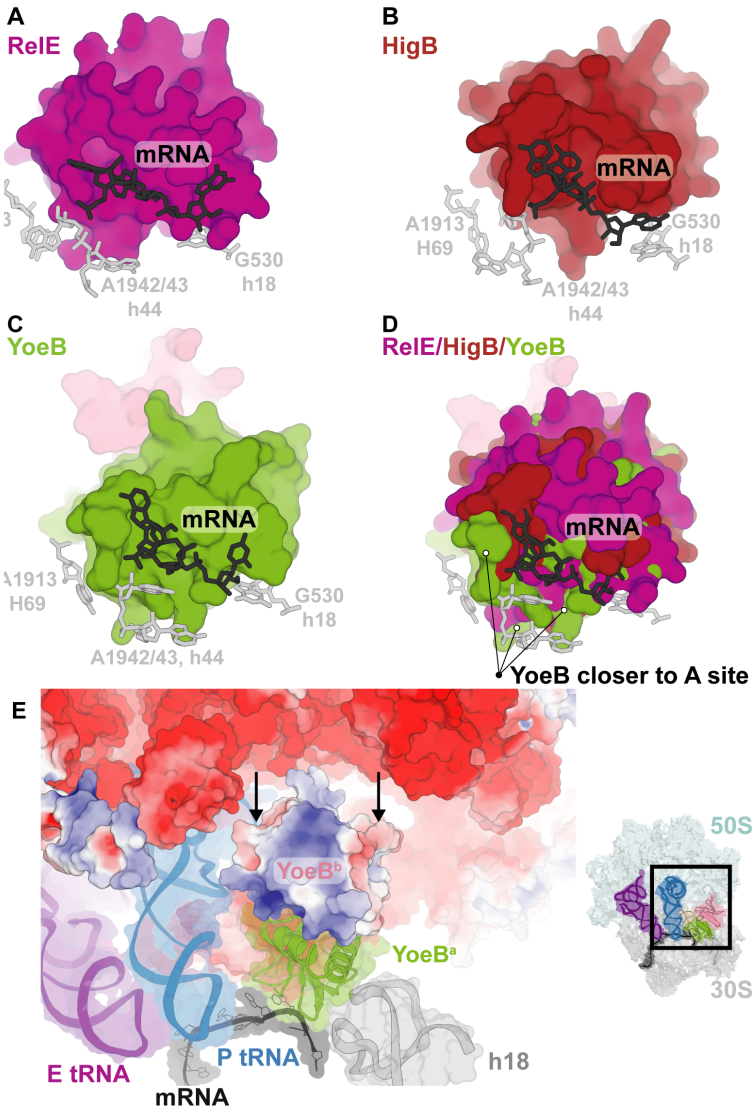

Figure S10. Figure S10. Size and electrostatic surrounding of YoeB help induce conformational changes in the A site. The positioning of **(A)** RelE (2), **(B)** HigB (1), **(C)** YoeB (this study; PDB ID 6OXA), or **(D)** RelE, HigB and YoeB in the A site surrounded by mRNA (black) and H69 residue A1913, h44 residues A1492 and A1493, and h18 G530 (gray) is shown. YoeB occupies more space close to A1913 and nucleotides A1492 and A1493 than any of the other toxins. **(E)** The electrostatic surface potential of YoeB^{b} and the 50S subunit are shown, where red and blue depict acidic and basic electrostatic potential respectively. Color scheme and inset is as in Figure S4. Two regions of overall negative charge on YoeB^{b} are repelled by the overall negative concave surface of the 50S ribosome. Electrostatic potential maps were generated using the Adaptive Poisson-Boltzmann Solver (APBS) plug-in (3) for PyMol version 2.3.1.

SUPPLEMENTARY TABLES

Table S1. Data collection and refinement statistics.

	30S-YoeB AAU (6-nt) pre-cleavage	70S-YoeB AAU (25-nt) pre-cleavage	70S-YoeB AAU (25-nt) post-cleavage	70S-YoeB UAA (25-nt) post-cleavage
Data Collection				
Space Group	P 4_1 2_1 2	P 2_1 2_1 2_1	P 2_1 2_1 2_1	P 2_1 2_1 2_1
Wavelength (Å)	0.9792	0.9795	0.9795	0.9795
Cell dimensions				
a, b, c (Å)	401.710, 401.710, 175.4400	212.791, 453.079, 608.934	213.364, 451.705, 607.630	214.676, 453.509, 609.501
α, β, γ (degrees)	90, 90, 90	90, 90, 90	90, 90, 90	90, 90, 90
Resolution (Å)	49.83-3.74 (3.87-3.74)	126.40-3.25 (3.37-3.25)	144.00-3.12 (3.23-3.12)	126.50-3.50 (3.62-3.50)
R_{pim} (%)	4.2 (48.5)	14.5 (74.0)	12.5 (75.9)	13.8 (70.7)
I/σI	11.11 (1.38)	6.05 (1.08)	6.60 (1.12)	5.98 (1.12)
Completeness (%)	97.21 (91.49)	93.43 (75.60)	98.56 (99.31)	98.03 (95.30)
Redundancy	3.3 (2.6)	3.3 (2.3)	3.7 (3.8)	3.2 (3.3)
$CC_{1/2}$	0.999 (0.673)	0.990 (0.348)	0.994 (0.370)	0.994 (0.373)
Refinement				
Reflections	143,160 (13,288)	854,004 (68,654)	1,014,860 (101,652)	729,071 (70,397)
R_{work}/R_{free} (%)	20.6/22.4	23.0/25.6	23.2/25.8	21.6/24.6
No. of atoms	53,249	298,432	298,517	295,153
B-factors (Å^2)				
Overall	171.02	88.93	80.57	101.81
Macromolecule	171.19	89.10	80.68	102.02
Ligand/ion	124.92	45.16	48.00	42.90
Root mean square deviations				
Bond lengths (Å)	0.008	0.006	0.009	0.007
Bond angles (degrees)	1.16	1.02	1.38	1.18

Data for the highest-resolution shell is shown in parentheses.

Table S2. Bacterial strains and plasmids used in this study.

Strain/plasmid	Description	Source
E. coli strain		
BL21-Gold(DE3)pLysS	F- ompT $hsdS_{\beta}(r_{\beta}\text{-}m_{\beta}\text{-})$ dcm^{+} Tet^{r} gal λ(DE3) endA Hte [pLysS Cam^{r}]	Agilent
BW25113	Δ(araD-araB)567 ΔlacZ4787(::rrnB-4) lacIp-400(lacIQ)λ- rpoS396(Am) rph-1 Δ(rhaD-rhaB)568 rrnB-4 hsdR514	(4)
Plasmid		
pBAD33	Expression vector with Cm^{r}-cassette, P_{BAD} promoter, pACYC184 origin, araC coding sequence, and ara operator	(5)
pBAD-*yoeB*	pBAD33 with *yoeB* gene (5'- NdeI/BamHI -3')	(6)
pBAD-*yoeB*(W5A)	pBAD33 with *yoeB*(W5A) gene (5'- NdeI/BamHI -3')	This paper
pBAD-*yoeB*(W5A·W10A)	pBAD33 with *yoeB*(W5A·W10A) gene (5'- NdeI/BamHI -3')	This paper
pET21c	Expression vector with Amp^{r}-casette, T7-promoter, pBR322 origin, lacI-coding sequence, lac operator	Novagen
pET21c-*yefM*-*yoeB*(his_6)	pET21c with *yefM* and C-terminal $(His)_6$-*yoeB* genes (5'- NdeI/XhoI -3')	(6)
pET21c-*yefM*-*yoeB*(his_6) (W5A)	pET21c with *yefM* and C-terminal $(His)_6$-*yoeB*(W5A) genes (5'- NdeI/XhoI -3')	This paper
pET21c-*yefM*-*yoeB*(his_6) (W5A·W10A)	pET21c with *yefM* and C-terminal $(His)_6$-*yoeB*(W5A·W10A) genes (5'- NdeI/XhoI -3')	This paper

Table S3. mRNAs used in this study.

mRNA	Sequence (5' to 3')
AAU (30S-pre)	AAU$A_mA_mA_m$
AAU (70S-pre)	GCCAAGGAGGUAAAAAUG$A_mA_mU_m$CAGA
AAU (70S-post)	GCCAAGGAGGUAAAAAUGAAUCAGA
UAA (70S-post)	GCCAAGGAGGUAAAAAUGUAACAGA

Underlined portions of sequences represent the A-site codon and a 2'-OCH_3 modification is depicted as a lower "m".

Table S4. Oligos used in site-directed mutagenesis for this study.

Oligo pair	Sequence (5' to 3')	Source
W5A, pBAD TM208_F t30g_g31c TM208_R t30g_g31c_R	ggagatatacatatgaaactaatcgcgtctgaggaatcatgggatgatt aatcatcccatgattcctcagacgcgattagtttcatatgtatatctcc	This study
W10A, pBAD TM0209c_F t45g_g46c TM0209c_R t45g_g46c_R	aactaatcgcgtctgaggaatcagcggatgattatctgtactg cagtacagataatcatccgctgattcctcagacgcgattagtt	This study
W5A, pET21c TM204_F, t305g_g306c TM204_R, t305g_g306c_R	gacattattgagtgaaactaatcgcgtctgaggaatcatgggatgatt aatcatcccatgattcctcagacgcgattagtttcactcaataatgtc	This study
W10A, pET21c TM205c_F, t320g_g321c TM205c_R, t320g_g321c_R	aactaatcgcgtctgaggaatcagcggatgattatctgtactg cagtacagataatcatccgctgattcctcagacgcgattagtt	This study
W5A/W10A, pET21c TM0220 TM0220_AS_pET21c	ggatccatatgaaactaatcgcgtctgagg tctcgctcgagataatgataacgacatgc	This study

References

1. Schureck, M.A., Dunkle, J.A., Maehigashi, T., Miles, S.J. and Dunham, C.M. (2015) Defining the mRNA recognition signature of a bacterial toxin protein. *Proc Natl Acad Sci U S A*, **112**, 13862-13867.

2. Neubauer, C., Gao, Y.G., Andersen, K.R., Dunham, C.M., Kelley, A.C., Hentschel, J., Gerdes, K., Ramakrishnan, V. and Brodersen, D.E. (2009) The structural basis for mRNA recognition and cleavage by the ribosome-dependent endonuclease RelE. *Cell*, **139**, 1084-1095.

3. Jurrus, E., Engel, D., Star, K., Monson, K., Brandi, J., Felberg, L.E., Brookes, D.H., Wilson, L., Chen, J., Liles, K. *et al.* (2018) Improvements to the APBS biomolecular solvation software suite. *Protein Sci*, **27**, 112-128.

4. Datsenko, K.A. and Wanner, B.L. (2000) One-step inactivation of chromosomal genes in Escherichia coli K-12 using PCR products. *Proc Natl Acad Sci U S A*, **97**, 6640-6645.

5. Guzman, L.M., Belin, D., Carson, M.J. and Beckwith, J. (1995) Tight regulation, modulation, and high-level expression by vectors containing the arabinose PBAD promoter. *J Bacteriol*, **177**, 4121-4130.

6. Zhang, Y. and Inouye, M. (2009) The inhibitory mechanism of protein synthesis by YoeB, an Escherichia coli toxin. *J Biol Chem*, **284**, 6627-6638.